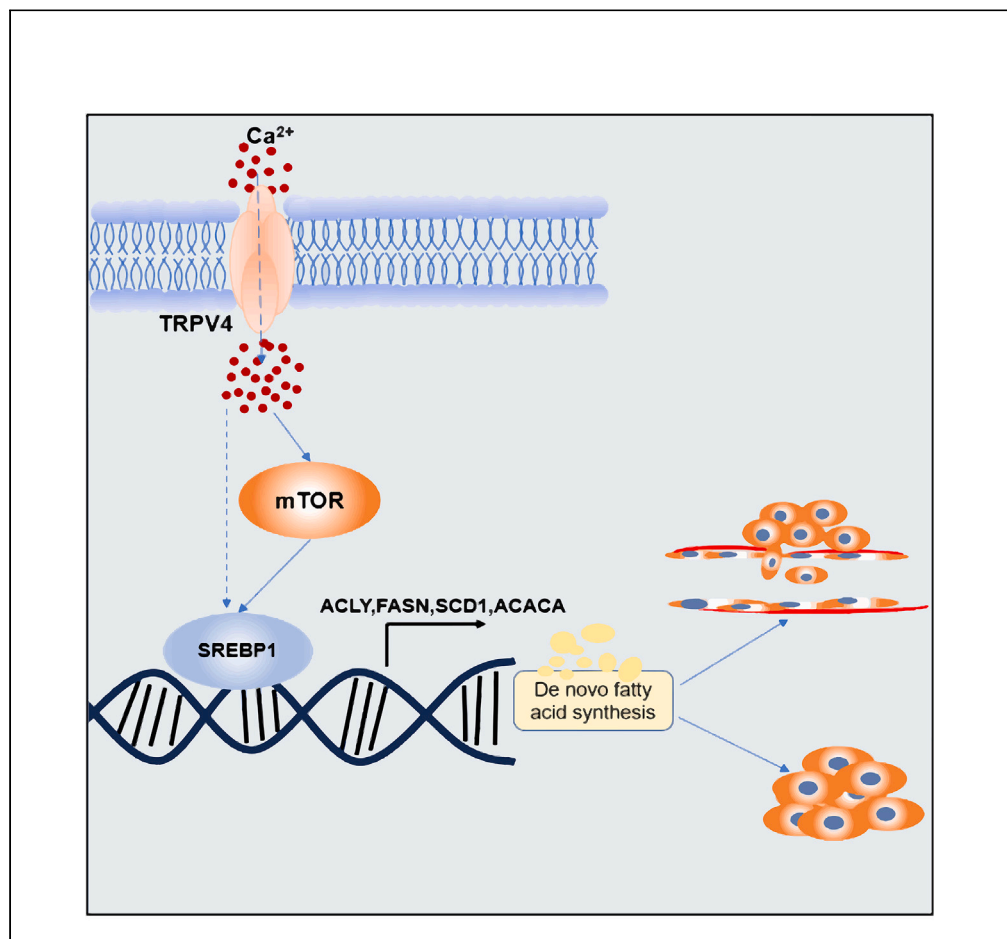


Article

TRPV4 enhances the synthesis of fatty acids to drive the progression of ovarian cancer through the calcium-mTORC1/SREBP1 signaling pathway



Lan Lin, Xiao Li, Ai-Jia Wu, Jia-bin Xiu, Yu-Zheng Gan, Xiao-mei Yang, Zhi-Hong Ai

xmyang@shsci.org (X.-m.Y.)
ai_zhihong@126.com (Z.-H.A.)

Highlights

TRPV4 plays an oncogenic role in ovarian cancer progression

Oncogenic pathway of TRPV4 may be related to the fatty acid synthesis in ovarian cancer

TRPV4 affects fatty acid synthesis through the calcium-mTORC1/SREBP1 signaling pathway

Article

TRPV4 enhances the synthesis of fatty acids to drive the progression of ovarian cancer through the calcium-mTORC1/SREBP1 signaling pathway

Lan Lin,^{1,3} Xiao Li,^{1,3} Ai-Jia Wu,^{1,3} Jia-bin Xiu,¹ Yu-Zheng Gan,¹ Xiao-mei Yang,^{2,*} and Zhi-Hong Ai^{1,4,*}

SUMMARY

Transient receptor potential vanilloid 4 (TRPV4) is a nonselective cation channel activated by various stimuli, such as heat. A recent study reported that high expression of TRPV4 predicted a poor prognosis in ovarian cancer patients. This study demonstrated that TRPV4 was highly expressed in ovarian cancer and had the ability to promote proliferation and migration. Through RNA-seq and related experiments, we confirmed that the oncogenic pathway of TRPV4 in ovarian cancer may be related to the fatty acid synthesis. By correlation analysis and RNA-seq, we demonstrated that SREBP1 and mTORC1 were inseparably related to that. Therefore, we used inhibitors to perform experiments. Calcium fluorescent probe experiments suggest that the change of calcium content in ovarian cancer cells was related to the downstream mTORC1 signaling pathway and fatty acid synthesis. These results confirmed that TRPV4 affected the fatty acid synthesis through the calcium-mTOR/SREBP1 signaling pathway, thereby promoting ovarian cancer progression.

INTRODUCTION

Globally, ovarian cancer is one of the most common gynecological malignancies, and its incidence rate is second only to cervical cancer and endometrial cancer; the mortality rate of female germ cell tumors is the highest.¹ Until 2018, ovarian cancer was the seventh most common malignant tumor in women worldwide, with approximately 240,000 new cases yearly.² Due to the lack of suitable screening methods and obvious symptoms,³ nearly 70% of patients have been diagnosed with advanced ovarian cancer stage.⁴ Therefore, it is of significant importance to study the pathogenesis of ovarian cancer and find new prognostic markers and therapeutic targets.

Transient receptor potential channel (TRP) is a non-voltage dependent cation channel mainly located on the plasma membrane, which generates signal transduction by changing the membrane potential and intracellular calcium ion concentration and responds to various signals inside and outside the cell such as temperature, pH and osmotic pressure stimuli, to occur corresponding physiological and pathological changes.⁵ Studies have shown that TRPCs, TRPM channels, and TRPV channels in the TRP channel family play essential roles in the occurrence and development of cancer.^{6–8} Transient receptor potential vanilloid 4 (TRPV4) belongs to the TRP family. As a nonselective cation channel, it can be activated by various stimuli, such as heat.⁹ TRPV4 is a member of the TRPV subfamily, widely distributed in the heart, brain, kidney, liver, lung, pancreas, and skin surface.¹⁰ TRPV4 channel protein is mainly localized on the plasma membrane and has six transmembrane regions, forming hairpin-like channels between the fifth and sixth transmembrane regions, allowing cations such as Ca²⁺ and Na⁺ to pass through.¹¹ Existing reports have reported that TRPV4 is highly expressed in colon, breast, gastric, and endometrial cancers and has different degrees of cancer-promoting effects.¹² Inhibit the expression of the TRPV4 gene in colon cancer, weaken intracellular Ca²⁺ influx, and interfere with the expression of D-type cyclin (cyclin D) through the PTEN pathway, affecting the progression of the cell cycle in the G1/S phase, thereby inhibiting the proliferation of colon cancer cells.¹³ Although TRPV4 is also highly expressed in ovarian cancer, its role in the progression of ovarian cancer and its molecular mechanism needs further exploration.

In cells, lipids regulate various life activities, and fatty acids are the main components of a variety of complex lipids.¹⁴ Unlike normal cells, almost all fatty acids in tumor cells come from the *de novo* synthesis process. Regardless of the extracellular and intracellular fatty acid levels, most tumor cells have a high rate of fatty acid synthesis.¹⁵ Studies have shown that many enzymes involved in fatty acid biosyntheses, such as ATP citrate lyase (ACLY), fatty acid synthase (FASN), acetyl coenzyme A carboxylase (ACACA), and stearyl coenzyme A desaturase 1 (SCD1), are highly expressed in many kinds of cancers and lead to poor prognosis.^{16,17} Previous research also found that fatty acid metabolism reprogramming is related to chemoresistance in ovarian cancer.¹⁸ During the process of lipid metabolism in ovarian cancer, the abnormal

¹Department of Gynecology and Obstetrics, Shanghai Sixth People's Hospital Affiliated to Shanghai Jiao Tong University School of Medicine, Shanghai 200233, China

²State Key Laboratory of Systems Medicine for Cancer, Shanghai Cancer Institute, Ren Ji Hospital, School of Medicine, Shanghai Jiao Tong University, Shanghai 200240, China

³These authors contributed equally

⁴Lead contact

*Correspondence: xmyang@shsci.org (X.-m.Y.), ai_zhihong@126.com (Z.-H.A.)

<https://doi.org/10.1016/j.isci.2023.108226>



expression of metabolic enzymes affects lipid synthesis or degradation, resulting in disordered lipid metabolism, thereby interfering with cancer development and energy supply.

The mTOR signaling pathway is a mechanistic channel with a wide range of functions in living organisms, and numerous studies have also confirmed that mTOR signaling could promote the anabolic process.¹⁹ mTORC1 enhances its central role in lipid biosynthesis by regulating the expression of multiple adipogenesis genes. Sterol regulatory element-binding proteins (SREBPs) are one of the critical transcription factor families involved in fatty acid synthesis. There is an inextricable relationship between mTOR signaling and SREBP1:²⁰ a group of studies found that a mTOR inhibitor prevents Akt-mediated accumulation of mSREBP1 in the nucleus and inhibits the induction of adipogenesis genes in epithelial cells.²¹

In our study, we used the GEO and TCGA databases to find that TRPV4 is highly expressed in OC and correlated with poor overall survival. At the same time, we found that the knockdown of TRPV4 suppressed the proliferation and migration of ovarian cancer cells *in vitro* and *in vivo*. RNA-seq revealed differential gene enrichment in the fatty acid synthesis pathway. We also confirmed this conclusion from the RNA, protein, fatty acid content levels, and correlation. Furthermore, we found that changes in intracellular calcium content, the critical transcription factors upstream of fatty acid synthesis (SREBP1), and the mTOR signaling pathway also participated in the cancer-promoting process. Our study demonstrated that TRPV4 promoted the carcinogenesis of ovarian cancer by mediating the calcium-mTORC1/SREBP1 pathway to upregulate fatty acid synthesis.

RESULTS

TRPV4 was upregulated in ovarian cancer tissues and related to poor prognosis

By analyzing several ovarian cancer datasets from GEO (GSE23391, GSE12470, GSE38666, and GSE40595) and taking $p < 0.05$ and $\log FC \geq 1.5$ as the screening criteria, 24 intersecting genes were obtained (Figure 1A). At the same time, we analyzed the dataset of TCGA ovarian cancer and the expression of TRPV4 in normal ovarian tissues in GTEX and found that the expression level of TRPV4 mRNA in ovarian cancer was significantly higher than that in normal tissues (Figure 1B). High TRPV4 mRNA expression was correlated with poor overall survival (OS: HR: 1.56, $p = 0.00081$) analyzed in the Kaplan-Meier plotter database (Figure 1C). RT-qPCR and western blot showed that the mRNA expression level and relative protein expression of TRPV4 in ovarian cancer cells were high, and the relative expression of TRPV4 protein in ovarian cancer tissues was higher than that in para-cancer tissue (Figure 1D). To confirm the increased expression of TRPV4 in ovarian cancers, we performed immunohistochemistry staining using an ovarian cancer microarray containing 106 cancer tissues and 15 normal tissues, and the results showed that TRPV4 was significantly upregulated in ovarian cancers ($p = 0.05$) (Figure 1E).

TRPV4 promoted ovarian cancer cell growth and migration

We investigated the biological role of TRPV4 in ovarian cancer. Hey and OV8 cells were silenced with siRNA or treated with HC067047, an antagonist to TRPV4. HO8910 cells were used to establish TRPV4 overexpression cell line using the lenti-TRPV4 virus. The successful knockdown or overexpression of TRPV4 was evidenced by RT-qPCR and western blot analysis (Figure 2A). Cell proliferation and the colony formation ability of ovarian cancer cells were suppressed by TRPV4 knockdown or HC067047 treatment, which were promoted by TRPV4 overexpression (Figures 2B and 2D). Transwell assays showed that knockdown of TRPV4 or blockage of TRPV4 with HC067047 significantly reduced while overexpression of TRPV4 increased cell migration through the 8 μm pore of the chamber, as compared to the control group (Figure 2C). These results demonstrated a promoting role of TRPV4 in ovarian cancer progression.

TRPV4 increased the expression levels of fatty acid synthesis enzymes in ovarian cancer cells

To investigate the underlying mechanism that mediates the tumor-promoting role of TRPV4, we knocked down TRPV4 expression in Hey cells with siRNA and then extracted RNA for sequencing. RNA-seq analysis revealed 1,706 differentially expressed genes, of which 824 were upregulated, and 882 were downregulated (p value < 0.05 , fold change > 2 and < 0.5) (Figure 3A). We found that the downregulated genes in the siRNA group vs. control group were significantly enriched in MYC, the mTORC1 pathway, oxidative phosphorylation, fatty acid metabolism, androgen response, and cholesterol homeostasis (Figure 3B). The significantly downregulated functions enriched by Gene Ontology were mainly related to the synthesis of intracellular biocomponents (Figure 3C). Fatty acid metabolism includes *de novo* synthesis, fatty acid oxidation, desaturation, and lengthening reactions.²² TRPV4 is a channel protein on the cell membrane, and the abnormal fatty acid content may affect the protein's function on the membrane. In studying the effect of cannabidiol (CBD) on human sebaceous gland function, researchers found that CBD could activate TRPV4 protein and affect lipid metabolism by interfering with the ERK1/2 MAPK signaling pathway, thereby inhibiting lipogenesis in blood lipid cells.²³ To study whether TRPV4 regulates *de novo* fatty acid synthesis, we analyzed the expression of the key enzymes in fatty acid synthesis (ACLY, FASN, ACACA, and SCD1). Our results showed that the mRNA and protein expression levels of these enzymes were significantly decreased in Hey and OV8 cells by TRPV4 knockdown, while reverse results were obtained in TRPV4-overexpressing HO8910 cell lines (Figures 3D and 3E). Furthermore, we found that intracellular free fatty acids and triglycerides were significantly decreased by TRPV4 knockdown in OV8 cells and increased by TRPV4 overexpression in HO8910 cells (Figure 3F). Spearman rank correlation analysis indicated a significant positive correlation between TRPV4 and ACLY ($r = 0.5$, $p < 0.001$), FASN ($r = 0.2$, $p < 0.001$), ACACA ($r = 0.4$, $p < 0.001$) and SCD1 ($r = 0.26$, $p < 0.001$) in TCGA database by GEPIA database (Figure 3G).

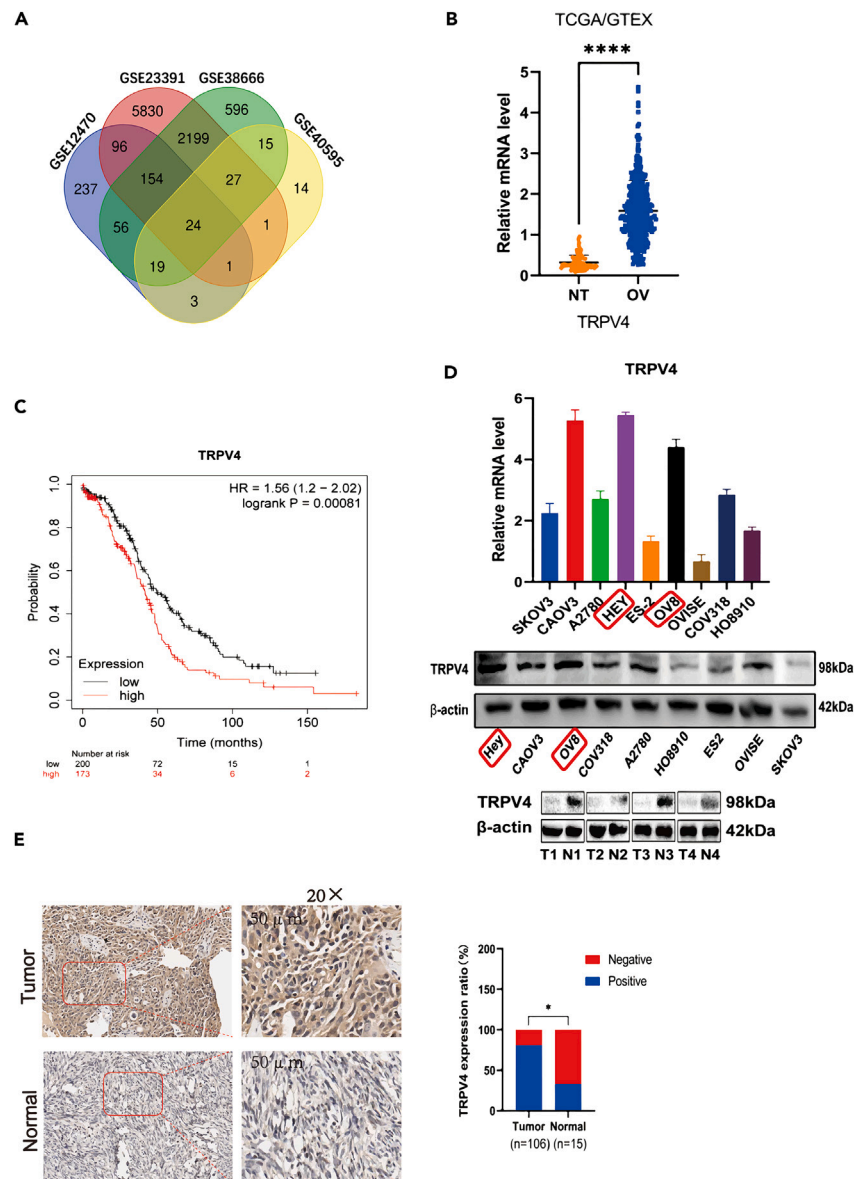


Figure 1. TRPV4 was upregulated in ovarian cancer tissues and related to poor prognosis

(A) Venn plot showing 24 genes including TRPV4 upregulated in GEO database GSE12470, GSE23391, GSE38666, and GSE40595.

(B) TRPV4 mRNA level in ovarian cancer tissues (OV) and normal ovarian cancer (NT) in TCGA and GTEX databases.

(C) Kaplan-Meier plot of the correlation between TRPV4 expression and patient survival.

(D) Upper panel: TRPV4 mRNA level in various ovarian cancer cell lines. Lower panel: TRPV4 protein level in various ovarian cancer cell lines and ovarian cancer tissues with ACTB detected as the internal control.

(E) Representative immunohistochemical images of TRPV4 expression and its normal tissues (lower). The constituent ratio of TRPV4 expression assessed by blinded IHC analyses in ovarian cancer tissues (n = 106) and normal tissues (n = 15) (lower). Scale bar indicates 50 μ m. *, p < 0.05; ****, p < 0.0001.

TRPV4 upregulated the expression of key enzymes to improve fatty acid synthesis via SREBP1

Sterol regulatory elementary binding protein 1c (SREBP1c) is an important transcription factor that regulates nascent fatty acid synthesis through transcriptional activation of lipogenic enzymes.^{24,25} Knockdown of SREBP1 can inhibit the growth of ovarian cancer *in vivo*, and enhancement can induce the reprogramming of tumor cell lipid metabolism and promote cancer cell proliferation and metastasis.²⁶ Through GEPIA database analysis, we found that SREBP1 (a key upstream transcription factor in fatty acid synthesis) strongly correlates with TRPV4 (Figure 4A). After the knockdown or overexpression of TRPV4, the expression of SREBP1 changed consistently with TRPV4 (Figures 4B and 4C). We confirmed that TRPV4 regulated fatty acid synthesis by holding SREBP1. HY-N0686, an inhibitor of SREBP1, was applied in the experiments. Four groups of cells expressing vector, OE, vector+HY-N0686, or OE + HY-N0686 were set up, and mRNA and protein were

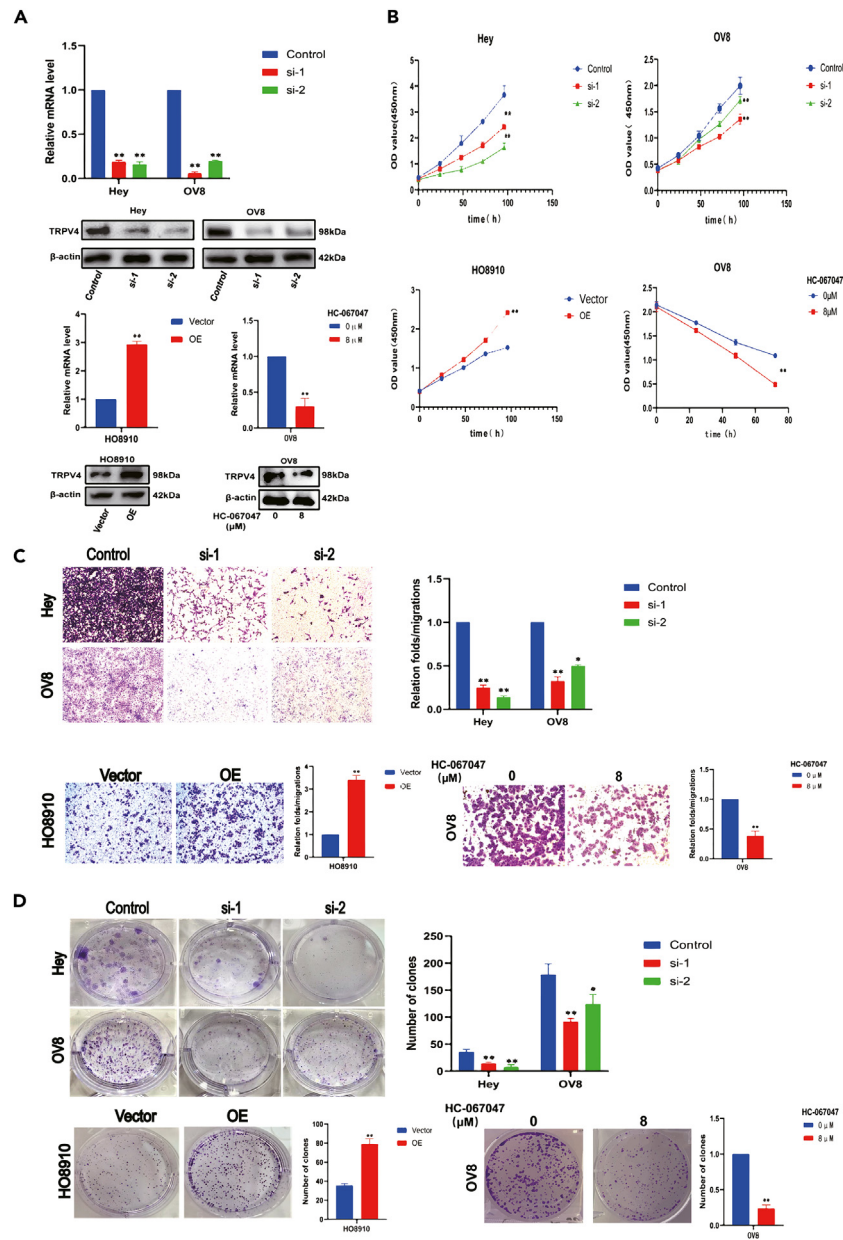


Figure 2. TRPV4 promoted the growth and migration of ovarian cells *in vitro*

(A) TRPV4 expression (silencing or overexpressing) in Hey, OV8, and HO8910 cells were verified by RT-qPCR analysis and western blotting. The effects of HC067047 on TRPV4 expression were also detected by qPCR and western blotting. si-1 and si-2, siRNAs against TRPV4; Control, scrambled siRNA; OE, expression vector encoding TRPV4; Vector, empty vector; HC067047, TRPV4 antagonist.

(B) Analysis of cell proliferation in ovarian cancer cells with TRPV4 knockdown, overexpression, or HC067047 treatment. Results were shown as the means \pm standard deviation of the OD 450 value.

(C) Representative images for transwell migration assays and statistical analysis (lower panel). Ovarian cancer cells with TRPV4 knockdown, overexpression, or HC067047 treatment were used. Scale bar:100 μ m.

(D) Anchorage-independent colony formation analysis of ovarian cancer cells with TRPV4 knockdown, overexpression, or HC067047 treatment. *, $p < 0.05$; **, $p < 0.01$; ***, $p < 0.001$.

extracted. Through qPCR and western blot, we found that the expression of SREBP1 was inhibited after HY-N0686 treatment. After overexpression of TRPV4, the upregulated expression of critical enzymes in fatty acid synthesis was reversed by HY-N0686 treatment ($p < 0.01$) (Figure 4D). Fatty acid content detection further demonstrated that TRPV4 overexpression promoted fatty acid levels, which were reversed by HY-N0686 treatment (Figure 4E). Further, the proliferation of ovarian cancer cells in the TRPV4 overexpression group was significantly reversed by

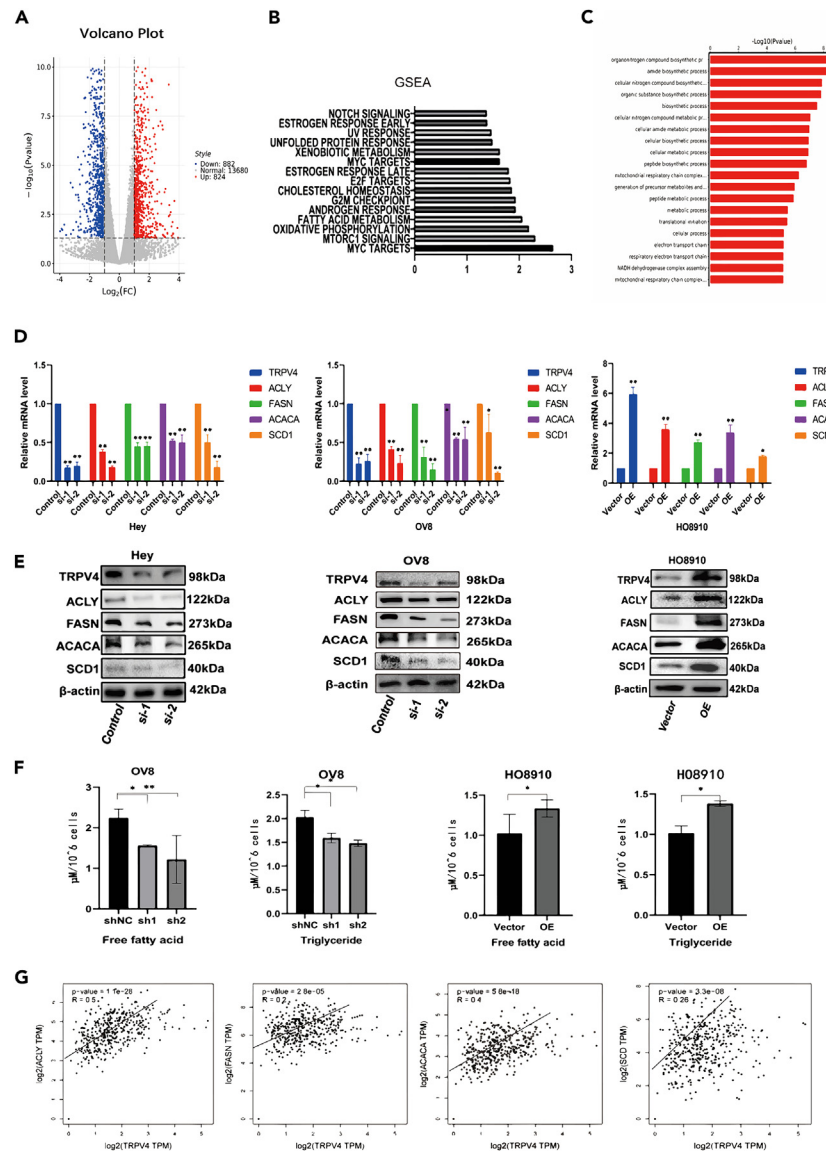


Figure 3. RNA-seq results and related experiment showed that TRPV4 increased the expression of fatty acid synthesis enzymes and promotes cellular free fatty acid level in ovarian cancer cells

(A) Volcano Plots: up-regulated genes were indicated by red dots (Foldchange > 2 and a p value ≤ 0.05) and down-regulated genes were indicated by green dots (Foldchange < 0.5 and p value < 0.05); gray dots indicated genes with no significant difference.

(B) Pathway KEGG database analysis, enriching differential genes and displaying them in bar graphs.

(C) GO enrichment of significantly downregulated genes in the siRNA group vs. control group by RNA-seq analysis.

(D and E) Quantitative RT-PCR and western blot analysis for mRNA and protein expression levels of *de novo* fatty acid synthesis enzymes of ACLY, FASN, ACACA, and SCD1 in Hey, OV8, and HO8910 cells with TRPV4 knocked-down or over-expression (N = 3).

(F) Cellular content of free fatty acid and triglyceride were detected in OV8 and HO8910 cells with TRPV4 knocked-down or over-expression as indicated.

(G) Spearman correlation analysis of the relationship between TRPV4 and fatty acid synthesis enzymes (ACLY, FASN, ACACA, and SCD1) in tumor tissues in TCGA ovarian cancer database. *, p < 0.05; **, p < 0.01; ***, p < 0.001.

SREBP1 inhibition, as detected by CCK8 and clone formation experiments (p < 0.01) (Figures 4F and 4G). SREBP1 inhibition with HY-N0686 also reversed cell migration as detected by the transwell experiments (Figure 4H).

TRPV4 promoted the expression of SREBP1 by activating the calcium-mTOR signaling pathway

Opened TRP channels can mediate Ca²⁺ influx and activate the Ca²⁺ signaling pathway, leading to cell proliferation, migration, apoptosis, and even death.²⁷ We used a fluorescent microplate reader to detect intracellular calcium ions. We found that the fluorescence intensity ratio

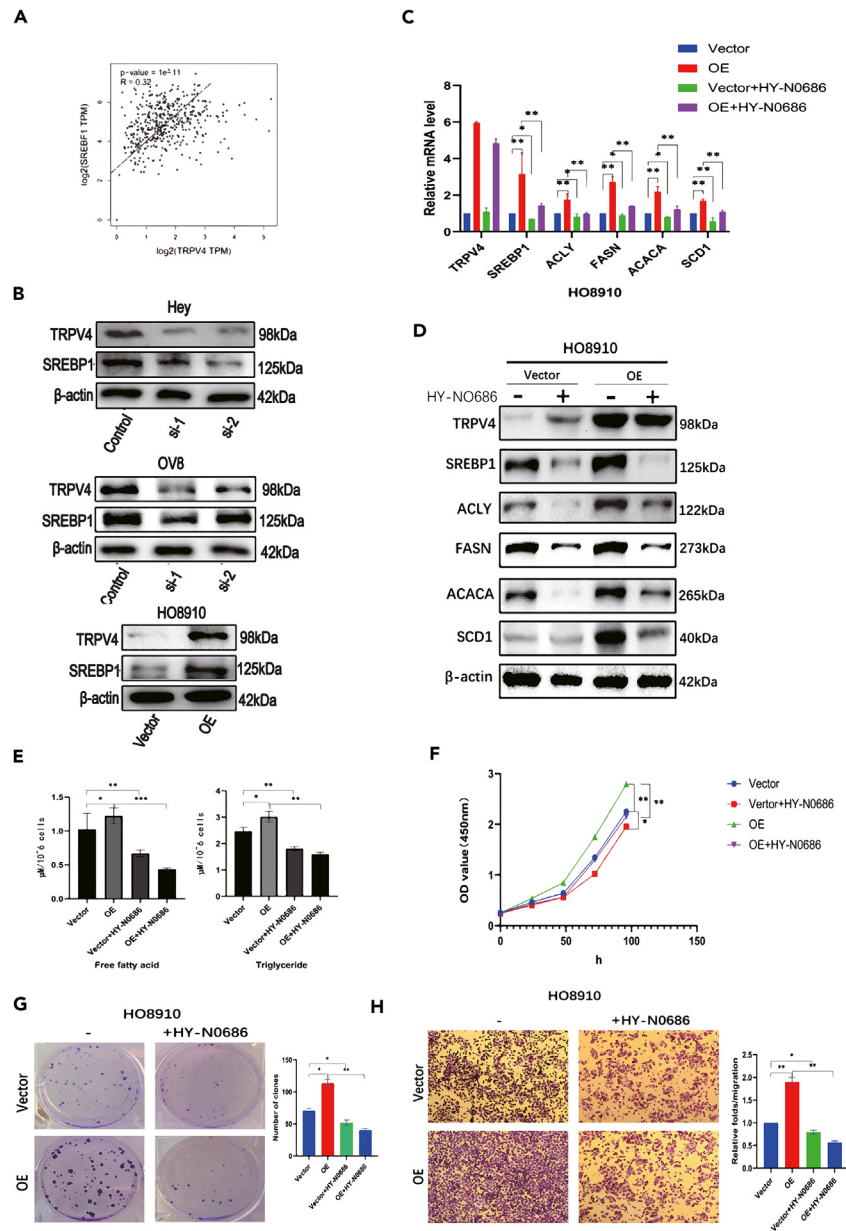


Figure 4. TRPV4 upregulated the key enzymes to improve fatty acid synthesis via SREBP1

(A) Spearman correlation analysis of the relationship between TRPV4 and SREBP1 in TCGA ovarian cancer database.

(B) Western blot analyses for expressions of SREBP1 in Hey, OV8, and HO8910 cells with treatment as indicated.

(C and D) Western blot expression and mRNA level of SREBP1, ACLY, FASN, ACACA, and SCD1 in HO8910 cells treated with a SREBP1 inhibitor (HY-N0686, 10 μ M SREBP1 inhibitor for 24 h).

(E) Cellular content of free fatty acid and triglyceride were detected in HO8910 treated with SREBP1 inhibitor.

(F–H) Cell proliferation and transwell migration were detected in HO8910 treated with SREBP1 inhibitor. *, $p < 0.05$; **, $p < 0.01$; ***, $p < 0.001$.

of intracellular calcium ions was significantly reduced by HC-067047, the inhibitor of TRPV4, with a dose-dependent manner ($p < 0.05$) (Figure 5A). Previous studies have found that TMBIM6 antagonists in B-cell lymphoma inhibit tumor formation and progression by preventing TMBIM6 from binding to mTOR and regulating calcium ion concentration, affecting protein synthesis and the expression of lipid synthesis genes.²⁸ mTOR signaling can regulate amino acid, glucose, nucleotide, fatty acid, and lipid metabolism.²⁹ Fatty acid synthesis and fatty acid uptake *in vivo* primarily respond to mTOR signaling. Studies have shown that the inhibition of mTORC1 can reduce the level of SREBP1, thereby significantly reduced lipid gene (such as ACLY, ACACA, FASN, and SCD1) expression.³⁰ By analyzing the GSEA enrichment results in RNA-seq, we found that the downregulated differentially expressed genes were remarkably enriched in the mTORC1 signaling

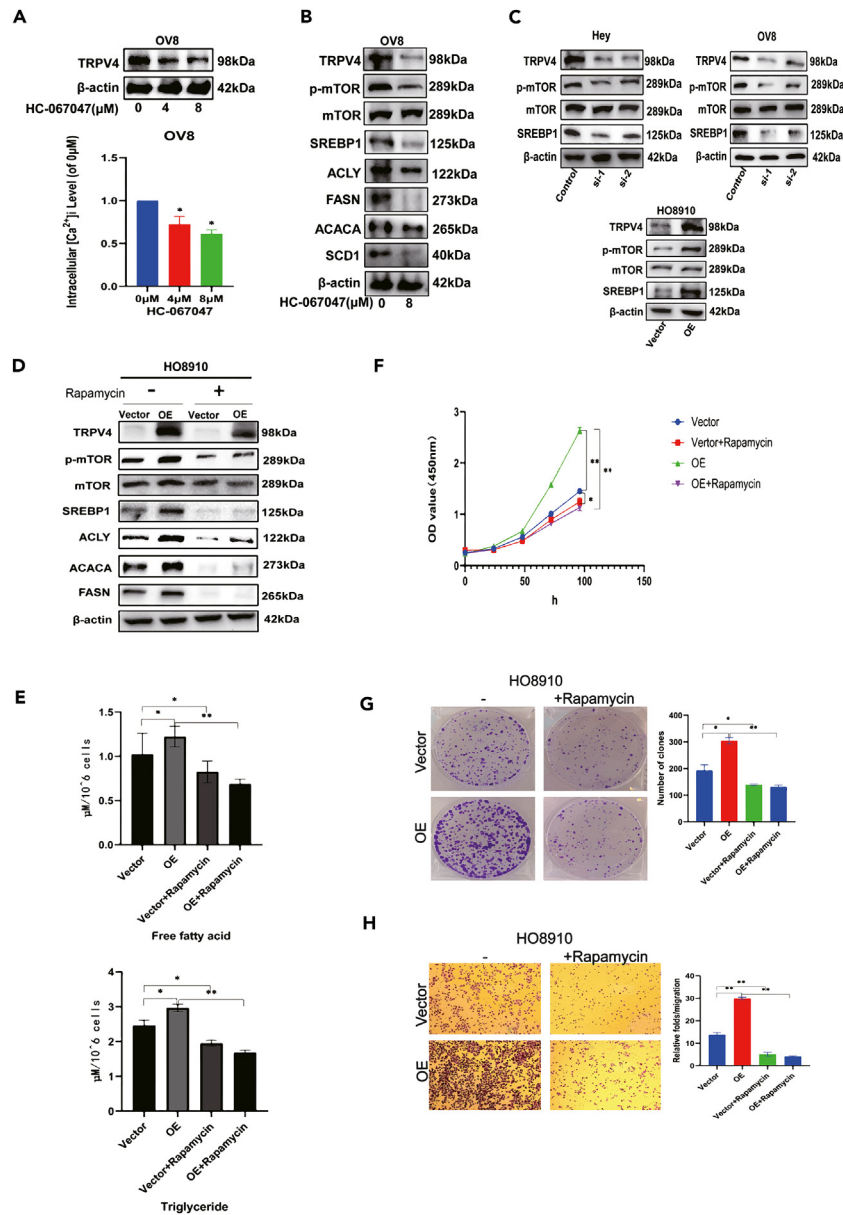


Figure 5. TRPV4 promoted the expression of SREBP1 and critical enzymes in fatty acid synthesis by activating the calcium-mTOR signaling pathway (A) Western blot analyses for expressions of TRPV4 treated with antagonist (0 μ M, 4 μ M, and 8 μ M); and changes in intracellular calcium concentrations in groups treated with different concentrations of antagonists. (B) Western blot analyses for protein expressions of TRPV4 and enzymes of *de novo* fatty acid synthesis in cells treated with antagonist HC-067047. (C) Western blot analyses for expressions of p-mTOR, mTOR and SREBP1 in Hey, OV8, and HO8910 cells with treatment as indicated. (D) Western blot analysis for expression of p-mTOR, mTOR, SREBP1 and key genes related to fatty acid synthesis in HO8910 cells treated with mTOR inhibitor (Rapamycin, 1 μ M inhibitor for 24 h). (E) Cellular content of free fatty acid and triglyceride were detected in HO8910 treated with mTOR inhibitor. (F–H) Cell proliferation and transwell migration were detected in HO8910 treated with mTOR inhibitor. *, $p < 0.05$; **, $p < 0.01$; ***, $p < 0.001$.

pathway (NES: -2.31 , NOM p -val < 0.001) (Figure 3B). For validation, mTOR signaling was detected by western blot in ovarian cancer cells. We found that the phosphorylation levels of mTOR and SREBP1 were decreased by TRPV4 blockage or knockdown, while they were increased by TRPV4 overexpression. The total level of mTOR was unchanged. Thus, mTOR may function downstream of TRPV4 (Figures 5B and 5C). Then, we applied rapamycin, an mTOR inhibitor, to TRPV4-overexpressing or control cells. The results showed that mTOR phosphorylation and SREBP1/2 expression were enhanced by TRPV4 overexpression, which was remarkably reversed by rapamycin (Figure 5D). In line with this finding, the expression of fatty acid synthesis enzymes was also clearly reduced after rapamycin treatment (Figure 5D). The fatty acid content

was consistently reduced by inhibition of mTOR signaling, as demonstrated in Figure 5E. Subsequent functional experiments, such as CCK8, clone formation, and transwell assays, showed that mTOR inhibition dramatically reversed the proliferation and migration of ovarian cancer cells enhanced by TRPV4 (Figures 5F–5H).

TRPV4 promoted ovarian cancer cell proliferation and migration by upregulating fatty acid synthesis *in vivo*

To further confirm the cancer-promoting effects of TRPV4, we used lenti-TRPV4 and lenti-vector cells in animal experiments. In the nude mouse xenograft model, tumor volumes and weights in mice injected with Hey-shNC cells were more significant than those in the Hey-sh1 group and Hey-sh2 group (Figures 6A and 6B). Immunohistochemistry results also showed that Ki67 positive cells were significantly decreased in tumors formed by TRPV4 knockdown cells *in vivo* (Figure 6C). By analyzing the subcutaneous tumor tissue of nude mice, we found that the free fatty acid and triglyceride contents in the knockdown group were lower than those in the vector group (Figure 6D). Immunohistochemical experiments further confirmed that the expression levels of fatty acid synthesis-related enzymes (SREBP1, FASN, and ACACA) in TRPV4 knockdown mice were lower than those in the vector group (Figure 6E). These results indicated that TRPV4 promoted ovarian cancer progression by regulating calcium-mTOR/SREBP1-mediated fatty acid synthesis (Figure 6F).

DISCUSSION

According to our country's 2015 cancer survey statistics, there were approximately 52,100 new cases of ovarian cancer in China.³¹ The five-year survival rate of patients with early-stage disease (stage I and II) after treatment is as high as 90%,³² while the survival rate of patients with advanced-stage disease (stage III and IV) is less than 30%.³³ Therefore, it is of great significance to study the mechanism of occurrence and development of ovarian cancer and to find effective intervention targets. In this study, by screening differentially expressed genes in public databases and analyzing the expression of the screened genes and their relationship with clinical prognosis, it was found that the TRPV4 channel protein gene may have a cancer-promoting effect in ovarian cancer. Then, IHC and western blot experiments confirmed that TRPV4 was highly expressed in ovarian cancer. Through a series of functional assays *in vitro* and *in vivo*, we found that TRPV4 could play a promoting role in ovarian cancer.

Studies have shown that the activation of *de novo* fatty acid synthesis in tumor cells is negatively correlated with the prognosis and disease-free survival of various types of tumors. This phenotype is mainly caused by the transcriptional, translational, and posttranslational modifications of lipogenesis-related genes, and the expression of these oncogenes is also affected by changes in lipid metabolism.¹⁶ The microenvironment of ovarian cancer is rich in a large number of adipocytes,³⁴ and enhanced *de novo* synthesis of fatty acids is a significant feature of cancer occurrence and development. Therefore, the lipid synthesis pathway may play an important role in ovarian cancer. In ovarian cancer stem cells, the synthesis of unsaturated fatty acids regulated by SCD1 has been shown to be critical for the proliferation and survival of cancer cells, and inhibiting its expression can delay the occurrence and development of tumors.³⁵ As cation channels, TRP channels have varying degrees of permeability to calcium ions, and calcium signaling has always played an important role in controlling lipid homeostasis.³⁶ TRPV1 is highly expressed on human epidermal and hair follicle keratinocytes, and studies have shown that its agonist (capsaicin) can regulate cell growth and death by affecting lipid homeostasis.³⁷ In leukemia, the morphology and function of adipocytes are critical for their development, while TRPV4 channel protein can induce adipocyte remodeling in residual bone marrow.³⁸ Using RNA sequencing, we revealed a close link between TRPV4 expression and the fatty acid synthesis process, which was subsequently validated by multiple experiments, including key enzyme detection and free fatty acid measurements. Nevertheless, whether TRPV4 regulates the fatty acid synthesis process through its function as a cation channel is still unknown. In this study, using fluorescence intensity measurements and western blot analysis, we demonstrated that TRPV4 was required for maintaining the intracellular calcium ion content and the expression of several enzymes critical for lipogenesis in ovarian cancer cells. Thus, the function of TRPV4 on fatty acid synthesis and tumor progression in ovarian cancer was largely related to its function as a calcium entry channel.

Transduction of oncogenic signaling and metabolic alterations are interconnected in cancer cells. mTOR signaling is often activated in cancer to control cell growth and metabolism. FASN is necessary for fatty acid synthesis, and in ovarian cancer, it inhibits the metabolic synthesis of cancer cells by inhibiting the PI3K-mTOR pathway.³⁹ The mTOR signaling pathway promotes lipid synthesis in cancer cells and mainly depends on downstream SREBP1/SREBP2. Studies have confirmed that SREBP1 is highly expressed in ovarian cancer and affects the growth of ovarian cancer by regulating downstream lipid production genes.⁴⁰ From the correlation analysis, we found that SREBP1, a key upstream transcription factor of fatty acid synthesis, was strongly correlated with TRPV4. From the sequencing results, we found that differentially expressed genes were enriched in signaling pathways such as mTORC1 and AMPK, which were inseparably related to fatty acid synthesis. Subsequent experiments using pathway-specific inhibitors confirmed that the TRPV4 channel protein affects the fatty acid synthesis process by modulating mTOR/SREBP1 signaling, thereby promoting the proliferation and migration function of ovarian cancer. We noticed that there was a slight change of TRPV4 protein level in HY-N0680-treated cells. We thought that SREBP1 inhibition by HY-N0680 might induce a feedback effect to increase TRPV4, while the underlying mechanism needs to be further investigated.

Current experimental results showed that TRPV4/calcium axis activated the mTOR signaling pathway to upregulate SREBP1 leading to enhanced fatty acid synthesis in ovarian cancer progression. As an ion channel, TRPV4 not only has certain permeability to calcium ions but also responds to stimuli such as pH, temperature, and mechanical stimulation *in vivo*. TRPV4 is a member of the TRP ion channel superfamily which can be activated by various physical or chemical stimuli.⁴¹ Phorbol ester compounds, and 5',6'-epoxyeicosatrienoic acid, a cytochrome p450 epoxygenase metabolite of arachidonic acid (AA), can activate TRPV4 in human hepatoblastoma cells.⁴² TRPV4 has also been proposed to have direct mechanosensing properties to mediate tumor metastasis.⁴³ The microenvironment of ovarian cancer is rich in adipocyte, thus it is possible that fatty acid from the microenvironment might contribute to the activation of TRPV4 in ovarian cancer cells.

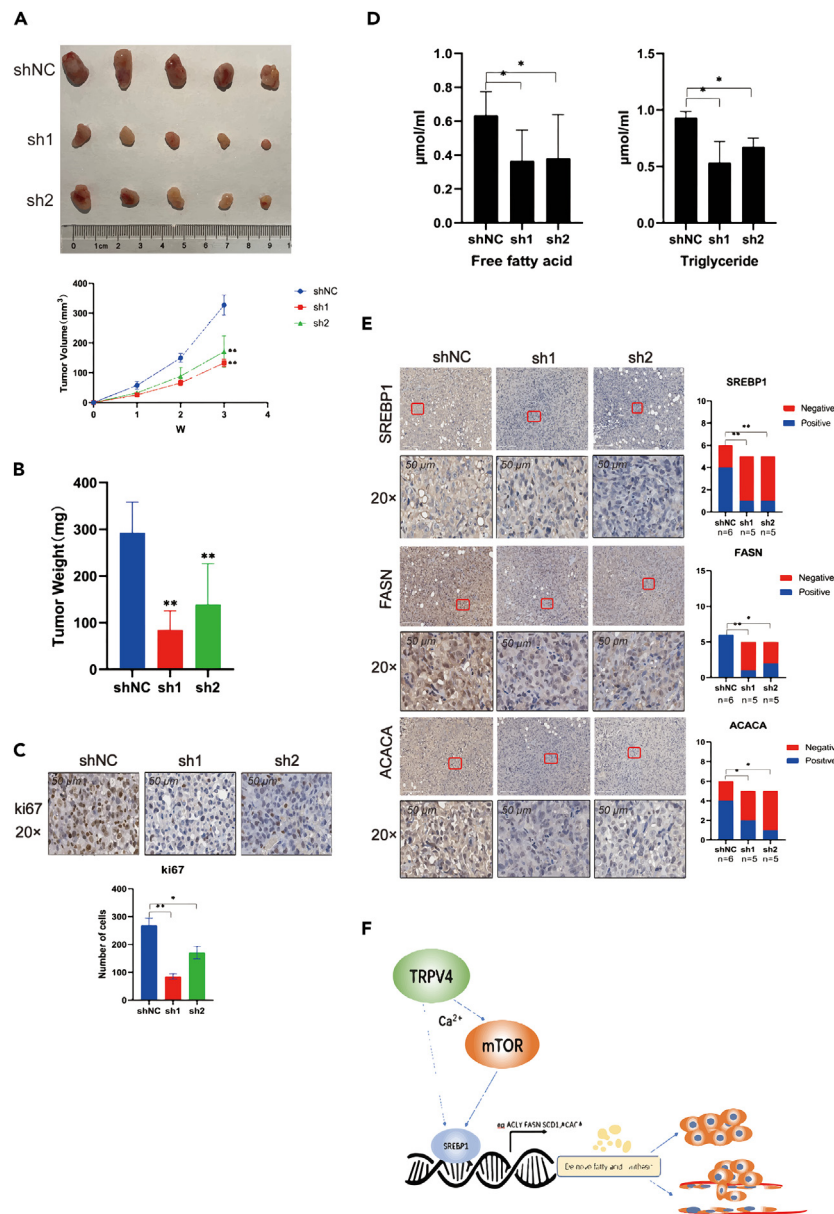


Figure 6. TRPV4 promoted the proliferation and migration of ovarian cancer cells by upregulating fatty acid synthesis in vivo

(A and B) Subcutaneous tumor growth in mice inoculated with Hey-sh1, Hey-sh2, and Hey-shNC cells. Each group of mice was randomly divided into 3 groups (n = 5 per group). (A) Photos of tumors and growth curve of tumors, (B) statistical analysis of tumor weight growth over 3 weeks. Data shown were the mean \pm standard deviation. p values were calculated by t test.

(C and E) Subcutaneous tumor tissues of nude mice were stained with ki67 and antibody (SREBP1, FASN, and ACACA), partial enlarged images of representative immunohistochemical images were selected. p values were calculated by t test.

(D) Free fatty acid content and triglyceride content of subcutaneous tumor in nude mice.

(F) TRPV4 enhanced synthesis of fatty acid to drive progression of ovarian cancer through calcium-mTOR/SREBP1 signaling pathway. *, p < 0.05; **, p < 0.01; ***, p < 0.001.

Therefore, whether the downstream mTOR-SREBP1 signaling pathway is activated by TRPV4 in response to the changes in the microenvironment of ovarian cancer is an interesting issue which needs to be further explored.

Limitations of the study

There are still many shortcomings in this study. First of all, the number of clinical samples collected is still small. Secondly, during this experimental process, we can analyze and study the effect of TRPV4 channel protein on the fatty acid synthesis process of ovarian cancer based on

clinical data. As an ion channel, TRPV4 not only has certain permeability to calcium ions, but also responds to pH value, temperature, mechanical stimulation, cytokines and other stimuli in the body. Therefore, in ovarian cancer, whether TRPV4 activates the downstream mTOR-SREBP1 signaling pathway in response to changes in the internal environment, thereby promoting fatty acid synthesis and enhancing cell proliferation and migration ability needs further exploration.

STAR★METHODS

Detailed methods are provided in the online version of this paper and include the following:

- [KEY RESOURCES TABLE](#)
- [RESOURCE AVAILABILITY](#)
 - Lead contact
 - Materials availability
 - Data and code availability
- [EXPERIMENTAL MODEL AND STUDY PARTICIPANT DETAILS](#)
 - Cell culture
 - Patient samples
 - Reagents and antibodies
 - Plasmid constructs
 - Mice
- [METHOD DETAILS](#)
 - Cell culture and tissue sample
 - Knockdown and overexpression of TRPV4
 - Quantitative real-time PCR analysis
 - Western blot assay
 - Cell proliferation and colony formation
 - Transwell assay
 - Immunohistochemistry (IHC)
 - RNA sequencing analysis
 - Quantification of free fatty acids and triglycerides
 - Measurement of intracellular calcium level ([Ca²⁺]_i)
 - Animal studies
- [QUANTIFICATION AND STATISTICAL ANALYSIS](#)
- [ADDITIONAL RESOURCES](#)

ACKNOWLEDGMENTS

This research was supported by the Natural Science Foundation of Shanghai (grant no. 22ZR1447300 to Dr Zhihong Ai). We thank Shanghai rainbow-genome company for technical support in RNA-seq.

AUTHOR CONTRIBUTIONS

L.L., X.L., and A.-J.W. developed the concepts, designed the experiments, and interpreted data. J.-B.X. partially contributed to the experiments presented in this article. Y.-Z.G. contributed to animal care and experiments. X.-M.Y. provided advice and technical assistance. L.L. and Z.-H.A. wrote and finalized the article. All authors read and approved the final article.

DECLARATION OF INTERESTS

The authors declare no competing interests.

INCLUSION AND DIVERSITY

We support inclusive, diverse, and equitable conduct of research.

Received: December 5, 2022

Revised: August 16, 2023

Accepted: October 13, 2023

Published: October 18, 2023

REFERENCES

- Bray, F., Ferlay, J., Soerjomataram, I., Siegel, R.L., Torre, L.A., and Jemal, A. (2018). Global cancer statistics 2018: GLOBOCAN estimates of incidence and mortality worldwide for 36 cancers in 185 countries. *CA. Cancer J. Clin.* 68, 394–424.
- Webb, P.M., Green, A.C., and Jordan, S.J. (2017). Trends in hormone use and ovarian cancer incidence in US white and Australian women: implications for the future. *Cancer Causes Control.* 28, 365–370.
- Goff, B.A., Mandel, L.S., Drescher, C.W., Urban, N., Gough, S., Schurman, K.M., Patras, J., Mahony, B.S., and Andersen, M.R. (2007). Development of an ovarian cancer symptom index: possibilities for earlier detection. *Cancer* 109, 221–227.
- Meyer, L.A., He, W., Sun, C.C., Zhao, H., Wright, A.A., Suidan, R.S., Dottino, J., Alejandro Rauh-Hain, J., Lu, K.H., and Giordano, S.H. (2018). Neoadjuvant chemotherapy in elderly women with ovarian cancer: Rates of use and effectiveness. *Gynecol. Oncol.* 150, 451–459.
- Li, H. (2017). TRP Channel Classification. *Adv. Exp. Med. Biol.* 976, 1–8.
- Liu, X., Zou, J., Su, J., Lu, Y., Zhang, J., Li, L., and Yin, F. (2016). Downregulation of transient receptor potential cation channel, subfamily C, member 1 contributes to drug resistance and high histological grade in ovarian cancer. *Int. J. Oncol.* 48, 243–252.
- Yang, S.L., Cao, Q., Zhou, K.C., Feng, Y.J., and Wang, Y.Z. (2009). Transient receptor potential channel C3 contributes to the progression of human ovarian cancer. *Oncogene* 28, 1320–1328.
- Han, G.H., Chay, D.B., Nam, S., Cho, H., Chung, J.Y., and Kim, J.H. (2020). Prognostic Significance of Transient Receptor Potential Vanilloid Type 1 (TRPV1) and Phosphatase and Tension Homolog (PTEN) in Epithelial Ovarian Cancer. *Cancer Genomics Proteomics* 17, 309–319.
- Clapham, D.E. (2003). TRP channels as cellular sensors. *Nature* 426, 517–524.
- Zhan, L., Yang, Y., Ma, T.T., Huang, C., Meng, X.M., Zhang, L., and Li, J. (2015). Transient receptor potential vanilloid 4 inhibits rat HSC-T6 apoptosis through induction of autophagy. *Mol. Cell. Biochem.* 402, 9–22.
- Suresh, K., Servinsky, L., Reyes, J., Baksh, S., Udem, C., Caterina, M., Pearse, D.B., and Shimoda, L.A. (2015). Hydrogen peroxide-induced calcium influx in lung microvascular endothelial cells involves TRPV4. *Am. J. Physiol. Lung Cell Mol. Physiol.* 309, L1467–L1477.
- Lee, W.H., Choong, L.Y., Mon, N.N., Lu, S., Lin, Q., Pang, B., Yan, B., Krishna, V.S.R., Singh, H., Tan, T.Z., et al. (2016). TRPV4 Regulates Breast Cancer Cell Extravasation, Stiffness and Actin Cortex. *Sci. Rep.* 6, 27903.
- Liu, X., Zhang, P., Xie, C., Sham, K.W.Y., Ng, S.S.M., Chen, Y., and Cheng, C.H.K. (2019). Activation of PTEN by inhibition of TRPV4 suppresses colon cancer development. *Cell Death Dis.* 10, 460.
- Huang, C., and Freter, C. (2015). Lipid metabolism, apoptosis and cancer therapy. *Int. J. Mol. Sci.* 16, 924–949.
- Wang, C., Ma, J., Zhang, N., Yang, Q., Jin, Y., and Wang, Y. (2015). The acetyl-CoA carboxylase enzyme: a target for cancer therapy. *Expert Rev. Anticancer Ther.* 15, 667–676.
- Currie, E., Schulze, A., Zechner, R., Walther, T.C., and Farese, R.V., Jr. (2013). Cellular fatty acid metabolism and cancer. *Cell Metab.* 18, 153–161.
- Wang, S., Fu, J.L., Hao, H.F., Jiao, Y.N., Li, P.P., and Han, S.Y. (2021). Metabolic reprogramming by traditional Chinese medicine and its role in effective cancer therapy. *Pharmacol. Res.* 170, 105728.
- Miranda, F., Mannion, D., Liu, S., Zheng, Y., Mangala, L.S., Redondo, C., Herrero-Gonzalez, S., Xu, R., Taylor, C., Chedom, D.F., et al. (2016). Salt-Inducible Kinase 2 Couples Ovarian Cancer Cell Metabolism with Survival at the Adipocyte-Rich Metastatic Niche. *Cancer Cell* 30, 273–289.
- Laplante, M., and Sabatini, D.M. (2012). mTOR signaling in growth control and disease. *Cell* 149, 274–293.
- Bakan, I., and Laplante, M. (2012). Connecting mTORC1 signaling to SREBP-1 activation. *Curr. Opin. Lipidol.* 23, 226–234.
- Porstmann, T., Santos, C.R., Griffiths, B., Cully, M., Wu, M., Leever, S., Griffiths, J.R., Chung, Y.L., and Schulze, A. (2008). SREBP activity is regulated by mTORC1 and contributes to Akt-dependent cell growth. *Cell Metab.* 8, 224–236.
- Athenstaedt, K., and Daum, G. (2006). The life cycle of neutral lipids: synthesis, storage and degradation. *Cell. Mol. Life Sci.* 63, 1355–1369.
- Oláh, A., Tóth, B.I., Borbó, I., Sugawara, K., Szöllösi, A.G., Czifra, G., Pál, B., Ambrus, L., Kloeppe, J., Camera, E., et al. (2014). Cannabidiol exerts sebostatic and antiinflammatory effects on human sebocytes. *J. Clin. Invest.* 124, 3713–3724.
- Wang, Y., Viscarra, J., Kim, S.J., and Sul, H.S. (2015). Transcriptional regulation of hepatic lipogenesis. *Nat. Rev. Mol. Cell Biol.* 16, 678–689.
- Yokoyama, C., Wang, X., Briggs, M.R., Admon, A., Wu, J., Hua, X., Goldstein, J.L., and Brown, M.S. (1993). SREBP-1, a basic-helix-loop-helix-leucine zipper protein that controls transcription of the low density lipoprotein receptor gene. *Cell* 75, 187–197.
- Cheng, X., Li, J., and Guo, D. (2018). SCAP/SREBPs are Central Players in Lipid Metabolism and Novel Metabolic Targets in Cancer Therapy. *Curr. Top. Med. Chem.* 18, 484–493.
- Sterea, A.M., Egom, E.E., and El Hiani, Y. (2019). TRP channels in gastric cancer: New hopes and clinical perspectives. *Cell Calcium* 82, 102053.
- Kim, H.K., Bhattarai, K.R., Junjappa, R.P., Ahn, J.H., Pagire, S.H., Yoo, H.J., Han, J., Lee, D., Kim, K.W., Kim, H.R., and Chae, H.J. (2020). TMBIM6/BI-1 contributes to cancer progression through assembly with mTORC2 and AKT activation. *Nat. Commun.* 11, 4012.
- Tee, A.R., Manning, B.D., Roux, P.P., Cantley, L.C., and Blenis, J. (2003). Tuberous sclerosis complex gene products, Tuberin and Hamartin, control mTOR signaling by acting as a GTPase-activating protein complex toward Rheb. *Curr. Biol.* 13, 1259–1268.
- Wang, B.T., Ducker, G.S., Barczak, A.J., Barbeau, R., Erle, D.J., and Shokat, K.M. (2011). The mammalian target of rapamycin regulates cholesterol biosynthetic gene expression and exhibits a rapamycin-resistant transcriptional profile. *Proc. Natl. Acad. Sci. USA* 108, 15201–15206.
- Chen, W., Zheng, R., Baade, P.D., Zhang, S., Zeng, H., Bray, F., Jemal, A., Yu, X.Q., and He, J. (2016). Cancer statistics in China, 2015. *CA Cancer J Clin* 66, 115–132.
- Chien, J., and Poole, E.M. (2017). Ovarian Cancer Prevention, Screening, and Early Detection: Report From the 11th Biennial Ovarian Cancer Research Symposium. *Int. J. Gynecol. Cancer* 27, S20–S22.
- Vargas, A.N. (2014). Natural history of ovarian cancer. *Ecanermedicalsience* 8, 465.
- Zhu, J., Wu, G., Song, L., Cao, L., Tan, Z., Tang, M., Li, Z., Shi, D., Zhang, S., and Li, J. (2019). NKX2-8 deletion-induced reprogramming of fatty acid metabolism confers chemoresistance in epithelial ovarian cancer. *EBioMedicine* 43, 238–252.
- Li, J., Condello, S., Thomes-Pepin, J., Ma, X., Xia, Y., Hurley, T.D., Matei, D., and Cheng, J.X. (2017). Lipid Desaturation Is a Metabolic Marker and Therapeutic Target of Ovarian Cancer Stem Cells. *Cell Stem Cell* 20, 303–314.e5.
- Berridge, M.J., Lipp, P., and Bootman, M.D. (2000). The versatility and universality of calcium signalling. *Nat. Rev. Mol. Cell Biol.* 1, 11–21.
- Tóth, B.I., Géczy, T., Griger, Z., Dózsa, A., Seltmann, H., Kovács, L., Nagy, L., Zouboulis, C.C., Paus, R., and Bíró, T. (2009). Transient receptor potential vanilloid-1 signaling as a regulator of human sebocyte biology. *J. Invest. Dermatol.* 129, 329–339.
- Yang, S., Lu, W., Zhao, C., Zhai, Y., Wei, Y., Liu, J., Yu, Y., Li, Z., and Shi, J. (2020). Leukemia cells remodel marrow adipocytes via TRPV4-dependent lipolysis. *Haematologica* 105, 2572–2583.
- Ediriweera, M.K., Tennekoon, K.H., and Samarakoon, S.R. (2019). Role of the PI3K/AKT/mTOR signaling pathway in ovarian cancer: Biological and therapeutic significance. *Semin. Cancer Biol.* 59, 147–160.
- Nie, L.Y., Lu, Q.T., Li, W.H., Yang, N., Dongol, S., Zhang, X., and Jiang, J. (2013). Sterol regulatory element-binding protein 1 is required for ovarian tumor growth. *Oncol. Rep.* 30, 1346–1354.
- Li, M., Zheng, J., Wu, T., He, Y., Guo, J., Xu, J., Gao, C., Qu, S., Zhang, Q., Zhao, J., and Cheng, W. (2022). Activation of TRPV4 Induces Exocytosis and Ferroptosis in Human Melanoma Cells. *Int. J. Mol. Sci.* 23, 4146.
- Vriens, J., Watanabe, H., Janssens, A., Droogmans, G., Voets, T., and Nilius, B. (2004). Cell swelling, heat, and chemical agonists use distinct pathways for the activation of the cation channel TRPV4. *Proc. Natl. Acad. Sci. USA* 101, 396–401.
- Hope, J.M., Greenlee, J.D., and King, M.R. (2018). Mechanosensitive Ion Channels: TRPV4 and P2X7 in Disseminating Cancer Cells. *Cancer J.* 24, 84–92.

STAR★METHODS

KEY RESOURCES TABLE

REAGENT or RESOURCE	SOURCE	IDENTIFIER
Antibodies		
TRPV4	Abcam	Cat# ab191580; RRID: N/A
ACTB(β -actin)	Proteintech (Wuhan, China)	Cat#20536-1-AP RRID: AB_10700003
ACLY	Proteintech (Wuhan, China)	Cat# 67166-1-Ig; RRID: AB_2882462
FASN	Proteintech (Wuhan, China)	Cat#10624-2-AP; RRID: AB_2100801
ACACA	Proteintech (Wuhan, China)	Cat#67373-1-Ig; RRID: AB_2882621
SREBP1	Proteintech (Wuhan, China)	Cat# 14088-1-AP; RRID: AB_2255217
mTOR	Proteintech (Wuhan, China)	Cat# 66888-1-Ig; RRID: AB_2882219
Phospho-mTOR (Ser2448)	Proteintech (Wuhan, China)	Cat# 67778-1-Ig; RRID: AB_2889842
SCD1	Abcam	Cat# ab39969; RRID: AB_945374
Anti-rabbit IgG, HRP-linked	Proteintech (Wuhan, China)	Cat# PR30011; RRID: N/A
Anti-mouse IgG, HRP-linked Antibody	Proteintech (Wuhan, China)	Cat# PR30012; RRID: N/A
Puromycin	Yeasen Biotechnology (Shanghai, China)	Cat# 60209ES60; RRID: N/A
Bacterial and virus strains		
Lentivirus	OBiO Technology (Shanghai, China)	N/A
Biological samples		
Human ovarian cancer and paired nontumor ovarian tissues	Servicebio company (Wuhan, China)	https://www.servicebio.cn/
Chemicals, peptides, and recombinant proteins		
Rapamycin	MedChemExpress	Rapamycin-HY-10219
Inhibitor of TRPV4	MedChemExpress	HC067047 (#HY-100208)
Inhibitor of SREBP1	MedChemExpress	HY-N0686
Critical commercial assays		
RNA-seq	Romics (Shanghai, China)	N/A
Deposited data		
RNA sequencing data for Hey upon TRPV4 knockdown expression	This paper	Accession number: PRJNA1021763 BioSample accessions: SAMN37570277 https://www.ncbi.nlm.nih.gov/sra/PRJNA1021763
Experimental models: Cell lines		
Human: Ov8	ATCC	https://www.atcc.org/
Human: Hey	ATCC	https://www.atcc.org/
Human: Ho8910	ATCC	https://www.atcc.org/
Experimental models: Organisms/strains		
Female BALB/c nude mice	The Laboratory Animal Center of Shanghai Jiao Tong University	N/A

(Continued on next page)

Continued

REAGENT or RESOURCE	SOURCE	IDENTIFIER
Oligonucleotides		
miRNAs targeting sequence for TRPV4	GenePharma (Shanghai, China)	N/A
siRNAs targeting sequence for TRPV4	GenePharma (Shanghai, China)	N/A
Primers for qRT-PCR	This paper	N/A
Recombinant DNA		
Plasmid: TRPV4-Flag	OBiO Technology (Shanghai, China)	N/A
Plasmid: TRPV4-Flag knockdown	OBiO Technology (Shanghai, China)	N/A
Software and algorithms		
GraphPad Prism9 Software	GraphPad	https://www.graphpad.com
Image J Software	National Institutes of Health (NIH)	https://imagej.nih.gov/ij/
Adobe Illustrator Software	Adobe	https://www.adobe.com/

RESOURCE AVAILABILITY**Lead contact**

Further information and requests for resources and reagents should be directed to and will be fulfilled by the lead contact, Zhi-Hong Ai (ai_zhihong@126.com).

Materials availability

This study did not generate new unique reagents.

Data and code availability

- The RNA-sequencing data is listed in the [key resources table](#).
- This paper does not report original code.
- Any additional information required to reanalyze the data reported in this paper is available from the [lead contact](#) upon request.

EXPERIMENTAL MODEL AND STUDY PARTICIPANT DETAILS**Cell culture**

The Ov8, Hey and Ho8910 cell lines were originally obtained from the American Type Culture Collection (ATCC, USA). All cells were all preserved in Shanghai Sixth People's Hospital Affiliated with Shanghai Jiao Tong University School of Medicine. All cell lines were cultured in DMEM (HyClone, MA, USA) supplemented with 10% fetal bovine serum (BI, Kibbutz Beit-Haemek, Israel).

Patient samples

An ovarian cancer chip (106 tumor tissue samples and 15 normal tissue samples) was purchased from Wuhan Servicebio company. Four pairs of ovarian cancer tissue samples and adjacent tissue samples (samples from the obstetrics and gynecology department of our hospital, all tissue samples were stored in liquid nitrogen after surgical resection, the Ethics Committee of our hospital approved this experiment, and all patients and their families agreed and signed informed consent). All ovarian cancer and normal tissue samples were collected from Chinese female.

Reagents and antibodies

The TRPV4 and SREBP1 inhibitor was purchased from MedChemExpress (China). SiRNAs and miRNAs targeting the open reading frames of TRPV4 were synthesized by GenePharma (Shanghai, China). Lentivirus was designed and produced by OBiO Technology (Shanghai, China). Cells were infected with lentivirus for 48 h and then selected with 2-5 $\mu\text{g}/\text{mL}$ puromycin for 48 h according to the manufacturer's instructions and plated again for further experiments. TRPV4 expression in ovarian cancer was determined using qPCR, WB and IHC experiments. All antibodies were purchased from commercial manufacturers, and detailed information is listed in the [key resources table](#).

Plasmid constructs

A plasmid overexpressing TRPV4-Flag was constructed by linking the full-length human TRPV4 cDNA with the GL186 pcSLenti-CMV-MCS-3FLAG-PGK-Puro-WPRE3 vector (OBiO Technology, Shanghai, China). A TRPV4-Flag knockdown plasmid was constructed by linking the

full-length human TRPV4 cDNA with the pSLenti-U6-shRNA (TRPV4)-CMV-EGFP-F2A-Puro-WPRE vector (OBiO Technology, Shanghai, China). The primer sequences used for plasmid construction are in the [method details](#).

Mice

Female BALB/c nude mice (4 week, 16g) were purchased from The Laboratory Animal Center of Shanghai Jiao Tong University (Shanghai, China) and housed under pathogen-free conditions. All *in vivo* experiments and protocols were approved by Shanghai Sixth People's Hospital Affiliated to Shanghai Jiao Tong University School of Medicine.

METHOD DETAILS

Cell culture and tissue sample

The human ovarian cancer cell lines (Ov8, Hey, Ho8910) were all preserved in Shanghai Sixth People's Hospital Affiliated with Shanghai Jiao Tong University School of Medicine. All cell lines were cultured in DMEM (HyClone, MA, USA) supplemented with 10% fetal bovine serum (BI, Kibbutz Beit-Haemek, Israel). An ovarian cancer chip (106 tumor tissue samples and 15 normal tissue samples) was purchased from Wuhan Servicebio company. Immunohistochemical staining was used to detect the expression of TRPV4 protein in ovarian cancer and normal ovarian tissues. We collected four pairs of ovarian cancer tissue samples and adjacent tissue samples (samples from the obstetrics and gynecology department of our hospital, all tissue samples were stored in liquid nitrogen after surgical resection, the Ethics Committee of our hospital approved this experiment, and all patients and their families agreed and signed informed consent). After grinding, the protein was extracted from the tissues for Western Blot detection.

The TRPV4 antibody was purchased from Abcam (USA). Pseudodiosgenin (PPD: HY-N0686, MCE) was used to inhibit the expression of SREBP1 and other fatty acid synthesis-related genes. Dissolve 5 mg of PPD powder in 970 μ l of DMSO solution to prepare a reagent with a concentration of 5mmol. When the number of cells in the six-well plate reached 80%, 2 μ l of PPD solution was added to 1mL of DMEM and incubated for 24 hours to collect the mRNA and protein. Rapamycin (Rapamycin-HY-10219) is a potent and specific mTOR inhibitor (1 μ l of inhibitor solution was added to 1mL of DMEM and incubated for 24 hours). TRPV4 specific inhibitor HC067047 (# HY-100208) was purchased from MedChem Express and dissolved in DMSO to 5 mM at -80°C .

Knockdown and overexpression of TRPV4

According to the manufacturer's operating procedures, the miRNAs targeting TRPV4 and the control miRNAs (GenePharma, Shanghai, China) were introduced into OC cells with a transfection reagent (Polyplus jetprime transfection). The sequence information for siRNAs is as follows: si-1 F: CCCACAUUGUCAACUACCU R: AGGUAGUUGACAAUGUGGGT; si-2: F: CUAUCCUCUUUGACAUCGUTT R: ACGA UGUCAAAGAGGAUAGTT. A plasmid overexpressing TRPV4-Flag was constructed by linking the full-length human TRPV4 cDNA with the GL186 pcSLenti-CMV-MCS-3FLAG-PGK-Puro-WPRE3 vector (OBiO Technology, Shanghai, China). A TRPV4-Flag knockdown plasmid was constructed by linking the full-length human TRPV4 cDNA with the pSLenti-U6-shRNA (TRPV4)-CMV-EGFP-F2A-Puro-WPRE vector (OBiO Technology, Shanghai, China). Lentivirus was produced by co-transfecting lentiviral plasmids and packaging plasmids into 293T cells. Cells were infected with lentivirus for 48 h and then selected with 2-5 $\mu\text{g}/\text{mL}$ puromycin for 48 h.

Quantitative real-time PCR analysis

According to the manufacturer's instructions, total RNA was extracted from OC cells using TRIzol (Invitrogen). Complementary DNA (cDNA) was synthesized by reverse transcription using transcriptional reverse transcriptase (Takara, RR036A, Japan). Quantitative real-time PCR (qRT-PCR) determined the gene expression level using 2 \times SYBR Green qPCR Master Mix. TRPV4 primers: 5'-TCAATGAACCTGCTGGGGA-CAAG-3' (forward), 5'-TGGTAGTAGGCGGTGAG AGTGAAG-3' (reverse).

Western blot assay

The antibodies used were anti-TRPV4 (Abcam, Cambridge, UK), ACTB (Proteintech, Wuhan, China), ACLY (Proteintech, Wuhan, China), FASN (Proteintech, Wuhan, China), ACACA (Proteintech, Wuhan, China), SREBP1 (Proteintech, Wuhan, China) and SCD1 (Abcam, Cambridge, UK). Ovarian cancer cells were treated with RIPA lysis buffer containing protease inhibitors to extract total protein. After quantification, protein loading buffer was added and boiled in boiling water for 7 minutes. According to the quantitative results, the corresponding amount of protein was added to the polyacrylamide gel, and electrophoresis was started. Then, the protein in the gel was transferred to a nitrocellulose membrane by the "sandwich" method. After blocking with 5% milk for 1 h, diluted antibody was added and incubated at 4°C overnight. TBST was washed three times (10 min) and then added with a secondary antibody to incubate at room temperature for 1 h, washed three times (10 min) with TBST. The results were analyzed with a chemical fluorescence imaging system.

Cell proliferation and colony formation

Cell proliferation was determined using a CCK-8 (Dojindo Laboratories, Kumamoto, Japan) assay. The 96-well plates were inoculated with 100 μL cell suspension of 2000 cells per well. Cells were transfected with siRNAs after attachment and cell viabilities were measured at 0h (before siRNA transfection), 24h, 48h, 72h and 96h post-transfection. 10% CCK8 in culturing medium was added to each well and incubated at 37°C for 1 hour. Absorbance at 450nm was measured using a Power Wave XS microplate reader (Infinite M100 pro, TECAN, Switzerland).

The experiment was performed in quintuplicate and repeated three times. For colony formation assay, single-cell suspension was plated at a density of 1,000 cells per plate in 6-well plates. The culture medium was changed every 3 days. After 21 days, colonies were fixed with 4% PFA (Beyotime, C0121), stained with crystal violet, and counted by microscopy.

Transwell assay

The migration assays were performed using a Transwell chamber (Millipore, Billerica, USA). Serum-free medium was used to suspend, count, and adjust the number of cells to 5×10^4 cells/ml. 200 μ L suspension was added to the upper chamber and 650 μ L medium containing 20% FBS was added to the lower chamber. Then, the plate was placed in the incubator for 24 hours. Cells that migrated through the pore were fixed and stained with crystal violet. The images were acquired using a light microscope with a magnification of 200 times. Statistical analyses were based on four independent experiments and analyzed with the Student's t-test.

Immunohistochemistry (IHC)

The slides were baked at 65°C for 30 minutes, dewaxed, and rehydrated in ethanol solutions. The endogenous peroxidase activity was quenched with 3% hydrogen peroxide for 10 minutes. The antigen was extracted by boiling the slide in the citric acid buffer for 20 minutes. After that, the slide was sealed in 4% BSA for 1 hour, incubated with the primary antibody at 4°C overnight, and labeled with HRP conjugated secondary antibody at room temperature for 1 hour. Then they were incubated with the DAB substrate (Thermo Scientific) and counterstained with hematoxylin. The primary antibodies used were anti-TRPV4 (Abcam, ab191580), anti-SREBP1 (proteintech, 14088-1-AP), anti-FASN (proteintech, 10624-2-AP) and anti-ACACA (proteintech, 67373-1-Ig). Protein staining was divided into positive and negative groups (no evident staining of tumor cells).

RNA sequencing analysis

The possible molecular mechanism was determined by RNA sequencing. TRIzol extracts total RNA from control, si-1 Hey cells. RNA-seq was performed by Romics (Shanghai, China). Gene expression was calculated by the FPKM method. The edgeR software package was used to analyze the difference in gene expression between groups. After calculating the value of p , multiple hypothesis tests were conducted to correct it. The threshold value of p is determined by controlling the error discovery rate (FDR). The Kyoto Encyclopedia of Genes and Genomes (KEGG) enriched differentially expressed genes.

Quantification of free fatty acids and triglycerides

Lipids were extracted from OC cell homogenate. OC cell homogenate was prepared by using chloroform/methanol (2:1). Then a free fatty acid and triglyceride kit (Bioassay Systems, Hayward, CA, USA) was used to quantitatively evaluate the levels of free fatty acids and triglycerides according to the manufacturer's instructions.

Measurement of intracellular calcium level ([Ca²⁺]_i)

The intracellular [Ca²⁺]_i concentration was measured with Fura-2/AM (Beyotime, S1052). The 96-well plate protecting from light was inoculated with 2.0×10^4 /100 μ L cell suspension. After the cells were adhered to the wall, they were incubated with the inhibitor HC-067047 or vehicle control for 30 min. Following, the cells were washed three times with PBS and incubated with medium containing 5 μ M Fura-2 AM at 37°C for 30 min. Then, the cells were washed 3 times with PBS and incubated for another 30 min. The fluorescence intensity was measured using a microplate reader with excitation and emission wavelengths of 340 and 510 nm, respectively.

Animal studies

The Laboratory Animal Center of Shanghai Jiao Tong University approved animal experiments. All animals received humane care according to the criteria outlined in the "Guide for the Care and Use of Laboratory Animals" prepared by the National Academy of Sciences and published by the National Institutes of Health. Female BALB/c nude mice (6 weeks old, 15–18 g) received a single subcutaneous flank injection of 1×10^8 TRPV4 knockdown Hey cells and control group cells ($n=5$ per group) in 150 μ L PBS. The tumor size was assessed each week. Three weeks after injection, the mice were sacrificed, and the tumors were harvested.

QUANTIFICATION AND STATISTICAL ANALYSIS

All experiments were repeated at least three times. Data were presented as mean \pm standard deviation. P values were calculated by t test and one-way ANOVA test by using GraphPad Prism9. $P < 0.05$ was considered as a significance level.

ADDITIONAL RESOURCES

The article does not have this section.